Astron. Astrophys. 222, 58–68 (1989)

ASTRONOMY
AND
ASTROPHYSICS

High-resolution polarization observations of M31

I. Structure of the magnetic field in the southwestern arm

R. Beck [1], N. Loiseau [1,2], E. Hummel [1,3], E.M. Berkhuijsen [1], R. Gräve [1,4] and R. Wielebinski [1]

[1] Max-Planck-Institut für Radioastronomie, Auf dem Hügel 69, D-5300 Bonn 1, Federal Republic of Germany
[2] Instituto de Pesquisas Espaciais, Departamento de Radioastronomia e Fisica Solar, C.P. 515, 12201 Sao José dos Campos, S.P., Brazil
[3] Nuffield Radio Astronomy Laboratories, Jodrell Bank, Macclesfield, Cheshire SK11 9DL, UK
[4] Max-Planck-Institut für Astronomie, Königstuhl, D-6900 Heidelberg 1, Federal Republic of Germany

Received January 12, accepted April 21, 1989

Summary. A region of the Andromeda galaxy (M 31) around the main spiral arm southwest of the nucleus was observed at λ 20.1 cm and λ 6.3 cm with the VLA and the Effelsberg radio telescope, respectively, both in total power and polarization. The radio emission is concentrated on a dust lane; the degrees of polarization are $\leqq$40% at λ 20.1 cm and $\leqq$60% at λ 6.3 cm.

The rotation measures (RM) and intrinsic magnetic field orientations (χ_B) confirm the model of a basic axisymmetric, nearly toroidal field in M 31. The existence of a superimposed bisymmetric spiral field cannot be investigated within the small region observed. However, periodic deviations from the basic axisymmetric field are visible in the intrinsic rotation measure (RM_i) and χ_B which also affect the degree of polarization. These deviations appear to have a scale length along the arm of $\sim$4.5 kpc and suggest the existence of a three-dimensional arc-like field structure, possibly a Parker-Jeans instability anchored in a large H I complex of $\sim$2 kpc length.

On the southern side of the centre of M 31 the magnetic field is generally aligned along the spiral structure seen in the ionized gas. On the northern side the emission at λ 20.1 cm is completely depolarized, possibly because of a filamentary or tangled structure of the magnetic field.

Key words: spiral galaxies: M 31 – radio continuum – polarization – Faraday rotation – interstellar magnetic fields

1. Introduction

The proximity of M 31 (D = 690 kpc) is the major advantage for studying the fine structure of its interstellar medium, although its high inclination (i = 78°) induces various problems. For instance, since the linear resolution on the minor axis is about 5 times worse than that on the major axis the ring-like structure at $\sim$10 kpc radius seen in most of its constitutuents (e.g. H I, Hα, FIR, UV) is partly due to insufficient resolution along the minor axis (e.g. Georgiev, 1988).

The first map of polarized radio emission of M 31, made at λ 11.1 cm with the 100-m Effelsberg radio telescope with an angular resolution of 4'.4 (Beck et al., 1980) showed that the polarized intensity is strongest in the bright "ring" of emission at $\sim$10 kpc from the centre.

This data was analyzed by Sofue and Takano (1981) and by Beck (1982) who found that the changes of intensity and position angle of the E-vectors with azimuthal angle were consistent with an axisymmetric, nearly toroidal magnetic field configuration. Recent λ 6.3 cm polarization observations (Berkhuijsen et al., 1987), which are nearly free of Faraday effects, give further support to an axisymmetric field structure.

The orientation of the E-vectors at λ 11.1 cm, after subtraction of the axisymmetric mode, shows a double-periodic variation with azimuthal angle which may be interpreted as Faraday rotation in a bisymmetric field super-imposed onto the basic axisymmetric component (Sofue and Beck, 1987). However, other kinds of systematic deviations from the ideal axisymmetric field could cause a similar effect. To study this further, data at at least one more frequency are needed to determine the essential parameters: the Faraday rotation measure (RM) and the intrinsic field direction in the plane of the sky.

Apart from a possible bisymmetric field component, the E-vectors at λ11.1 cm show scatter which might be due to local changes of the RM. The causes for such changes could be changes of the magnetic field strength or direction, clumping of the thermal electrons or variations in the path length. All these factors point to the need of observations with high angular resolution.

The region of maximum polarized emission and maximum degree of polarization at λ 11.1 cm (Beck et al., 1980), near the minor axis southwest of the nucleus, was chosen for the first VLA measurements of polarized emission from M 31. The final resolution of 75″ is sufficient to resolve features of $\sim$250 pc along the major axis (i.e. in the azimuthal direction or along the "ring") and $\sim$1.2 kpc along the minor axis (i.e. in the radial direction). Preliminary results have been published by Loiseau et al. (1987).

2. Observations and data reduction

We observed the total and the linearly polarized radio emission at λ 20.1 cm from a selected region in M 31 with the Very Large Array

Send offprint requests to: R. Beck

(VLA) of the National Radio Astronomy Observatory (NRAO) [1] in its most compact configuration (D-array) for 4 hours (excluding time used for calibration). The field was centered at RA = $00^h38^m36^s$, DEC = 40°54′ (1950.0) were earlier measurements (Beck et al., 1980) showed the highest degree of polarization.

The observations were done at two independent IFs, each with a band-width of 50 MHz, and separated by 50 MHz. These two IFs were combined after checking that this did not enhance the bandwidth depolarization. The final central frequency is 1.49 GHz and the bandwidth is 100 MHz. The flux density scale was calibrated by observing 3 C 48 for which we assumed a flux density of 15.6 Jy. The position angle of the linearly polarized emission was calibrated by observing 3 C 138 for which we assumed a value of 168°. The phase calibrator 0038+328, whose position is known with an accuracy of ~0″.2, was also used to correct for the instrumental polarization.

The edited and calibrated visibility data were Fourier transformed to obtain maps of the Stokes parameters I, Q, and U. In this map making procedure the sidelobes of the synthesized beam were removed. The full resolution maps so obtained have a synthesized beam with a half power beamwidth (HPBW) of ~40″. Because of the low linearly polarized intensity we applied a weighting function to the visibility data so that the resulting HPBW became 75″. The Q and U maps were combined to obtain maps of the linearly polarized emission (corrected for the positive zero level offset) and of the position angle of the electric vectors (E-vectors).

The primary beam of the VLA has a HPBW ~30′ so we could only study a small part of M 31. In addition our measurements are, because of the minimum spacing of 40 m, insensitive to larger scale structures. Gaussian structures with a half power size of $\gtrsim$12′ have a visibility of $\lesssim$0.2 and are not properly mapped.

3. Results

The maps of the total and linearly polarized intensity are presented in Figs. 1 and 2. The resolution of 75″ corresponds to 250 × 1200 pc in the plane of the galaxy. Several background sources are strongly polarized (Table 1). The errors given in Table 1 are the uncertainties in the Gaussian fits and do not include the uncertainty of the calibration scale which is < 5%. The ambiguity in RM was solved with the help of the λ 11.1 cm data of Beck et al. (1980). Table 1 shows that the RM of sources within ~10′ from the spiral arm of M 31 vary considerably. These variations do not follow the deviations of RM_i in Fig. 7 and may be intrinsic to the sources.

Both the total emission (Fig. 1) and the linearly polarized emission (Fig. 2) very closely follow the dust lane that runs just outside the most conspicuous optical spiral arm in this region. The continuum ridge also coincides with the ridges seen in other constituents like H I (Brinks and Shane, 1984), H II regions (Pellet et al., 1978), and FIR emission (Walterbos and Schwering, 1987). The inner and outer arms could not be detected. The degree of polarization is between 10% and 20% on the dust lane, but reaches values up to 40% at the edges of the optical spiral arm. The central region of M 31 extends over more than 10′. The peak flux density of the nucleus (after correction for primary beam attenuation) is 27 mJy/beam and the degree of polarization is 2.3 ± 0.4%.

[1] The NRAO is operated by Associated Universities, Inc., under contract with the National Science Foundation.

Table 1. Polarized sources in the M 31 field

Name 37 W	Name 5 C 3.	S_{20} (mJy)	$S_{p,20}$ (mJy)	p_{20} (%)	ψ_{20} (°)	S_6 (mJy)	$S_{p,6}$ (mJy)	p_6 (%)	ψ_6 (°)	$\alpha^{20.1}_{6.3}$	RM (rad m^{-2})
45	73	73 ± 2	6.7 ± 0.2	9.2 ± 0.4	68 ± 1	26 ± 4	2.5 ± 1.0	10 ± 4	110 ± 11	0.89 ± 0.13	−106 ± 5
50	77	48 ± 2	3.7 ± 0.2	7.7 ± 0.6	159 ± 2	15 ± 1	2.4 ± 1.2	16 ± 8	154 ± 14	1.00 ± 0.07	− 84 ± 7
57	83	31 ± 1	1.5 ± 0.1	4.8 ± 0.4	75 ± 2	8 ± 1	< 1.5	< 19	–	1.17 ± 0.11	–
74 A/B	90	20 ± 1	2.2 ± 0.2	11.0 ± 1.1	96 ± 3	6 ± 2	1.8 ± 0.7	30 ± 12	135 ± 11	1.04 ± 0.29	−105 ± 5
89	96	29 ± 1	3.3 ± 0.4	11.4 ± 1.4	180 ± 3	14 ± 2	2.2 ± 1.0	16 ± 7	144 ± 13	0.63 ± 0.13	− 69 ± 6
91	97	54 ± 1	2.2 ± 0.1	4.1 ± 0.2	122 ± 1	24 ± 2	2.6 ± 1.0	11 ± 4	25 ± 11	0.70 ± 0.07	− 40 ± 5
94	98	48 ± 1	1.0 ± 0.2	2.1 ± 0.4	43 ± 6	13 ± 2	< 1.5	< 12	–	1.13 ± 0.13	–
115	107	306 ± 14	16 ± 2	5.2 ± 0.7	41 ± 4	115 ± 15	4.3 ± 0.7	3.7 ± 0.8	80 ± 5	0.84 ± 0.12	−105 ± 3

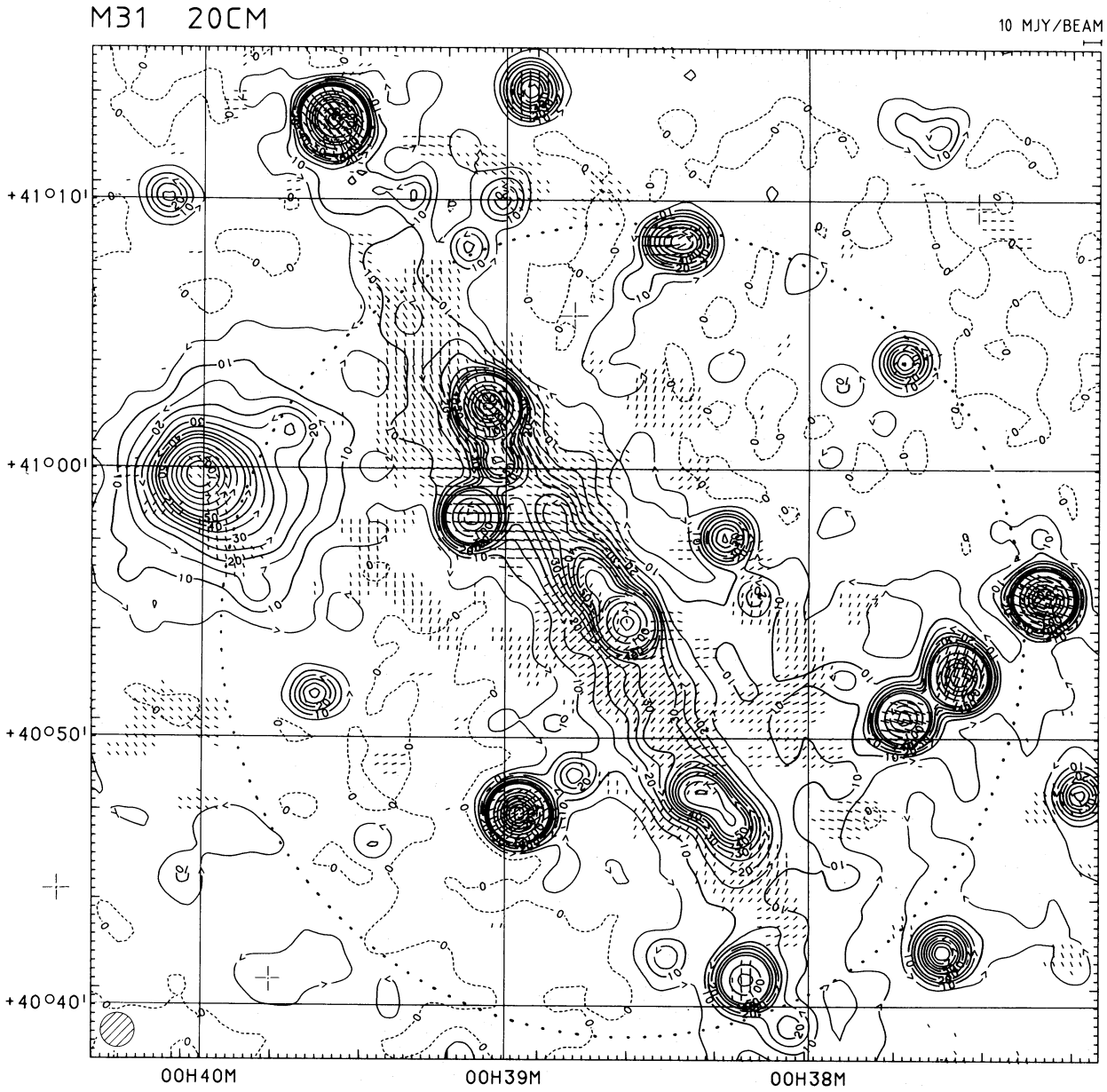

Fig. 1. Total radio continuum emission from the SW spiral arm of M 31 at λ20.1 cm. Contour levels are 0, 5, 10, . . . , 50, 60, . . . , 100, 150, . . . , 300, 400, 500, . . . in units of 0.1 mJy/beam. The half-power beamwidth of the synthesized beam is 75″ and is shown in the lower left-hand corner. The rms noise is 0.07 mJy/beam. The dotted circle indicates the half-power beamwidth of the primary beam. The lengths of the *E*-vectors indicate the flux density of the linearly polarized emission

Faraday rotation measures (RM) between λ20.1 cm and λ6.3 cm were obtained by comparison with the Effelsberg data of Berkhuijsen et al. (1987) (Figs. 3 and 4), after both data sets had been smoothed to a Gaussian beamwidth of 3′. All values above 2 times the rms noise were used to compute a map of RM (Fig. 5). The RM ambiguity due to the $\pm n \cdot 180°$ – ambiguity of the polarization angles was solved with the help of the λ11.1 cm map of Beck et al. (1980). The map of rotation measures will be discussed in detail in Paper II (Berkhuijsen and Beck, in preparation).

The rotation measures of Fig. 5 allow the correction of the orientations of the *E*-vectors in Fig. 4 to intrinsic polarization angles. These were then rotated by 90° so that they indicate the orientations of the magnetic field lines in the plane of the sky ($B_\perp$) (Figs. 5 and 6). The field lines generally follow the dust lane outside the main optical arm. Systematic deviations are discussed in the following Section.

4. Deviations from the axisymmetric magnetic field

Average rotation measures were obtained by separately averaging the Stokes Q and U maps at λ20.1 and λ6.3 cm in sectors of rings in 4 radius intervals (6–8, 8–10, 10–12, 12–14 kpc) (Fig. 7). A foreground RM of -88 rad m^{-2} was subtracted (see below). The observations cover the range of azimuthal angle $\theta = 60°$–$100°$ in the plane of the galaxy, counted anticlockwise from the SW major axis (see also Fig. 4).

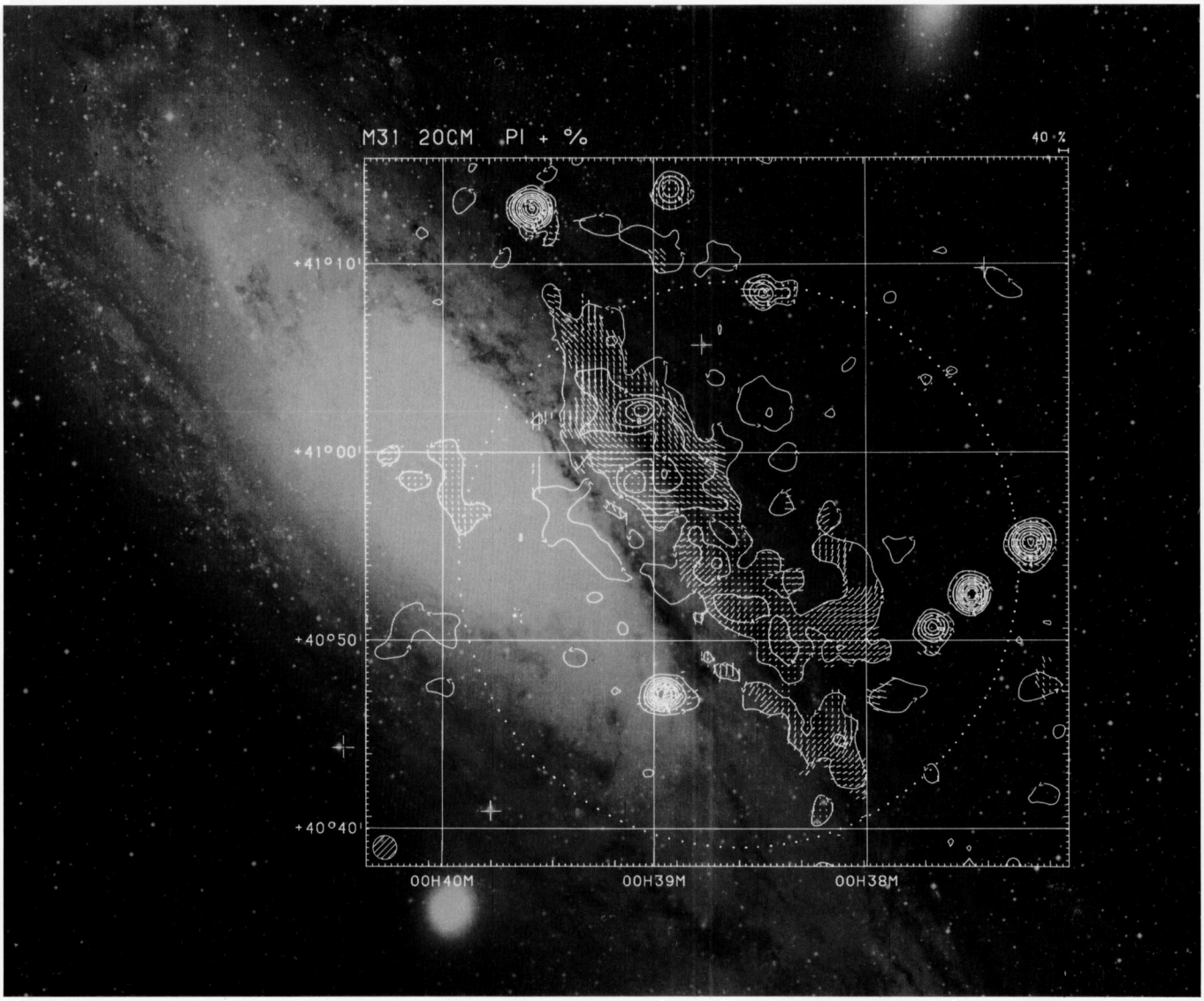

Fig. 2. Linearly polarized emission from the SW spiral arm of M 31 at λ20.1 cm overlayed onto an optical photograph of the Hale Observatories. Contour levels are 2, 4, 8, ... in units of 0.1 mJy/beam. The half-power beamwidth of the synthesized beam is 75″. The rms noise is 0.04 mJy/beam. The dotted circle indicates the half-power beamwidth of the primary beam. The lengths of the *E*-vectors indicate the degree of linear polarization. The degree of polarization was computed at all points with total intensity values above 3 times the rms noise and polarized intensity values above 2 times the rms noise

In the axisymmetric magnetic field model the RM varies with azimuthal angle θ as:

$$\mathrm{RM} = \mathrm{RM_i} + \mathrm{RM_{fg}} = \mathrm{RM_{max}} \cos(\theta + \phi) + \mathrm{RM_{fg}}\,, \qquad (1)$$

where $\mathrm{RM_i}$ is the rotation measure internal to M 31, $\mathrm{RM_{fg}}$ the rotation measure of the Galactic foreground and $\mathrm{RM_{max}}$ is the maximum rotation measure near the major axis. ϕ is a phase shift due to a systematic pitch angle of the magnetic field lines with respect to the model-ring (see Krause et al., 1989). The model curves indicated in Fig. 7 were calculated from the values for $\mathrm{RM_0}$, $\mathrm{RM_{fg}}$ and ϕ determined by Beck (1982) based on the λ11.1 cm observations. The internal rotation measures are expected to increase smoothly from $\mathrm{RM_i} \simeq -30\,\mathrm{rad\,m^{-2}}$ at $\theta = 100°$ to $\mathrm{RM_i} \simeq +30\,\mathrm{rad\,m^{-2}}$ at $\theta = 60°$. A superimposed BSS field (Sofue and Beck, 1987) would flatten this increase to $\mathrm{RM_i} \simeq -20\,\mathrm{rad\,m^{-2}}$ at $\theta = 100°$ and $\mathrm{RM_i} \simeq +20\,\mathrm{rad\,m^{-2}}$ at $\theta = 60°$. However, the values of $\mathrm{RM_i}$ in Fig. 7 only partly follow the predicted increase.

Could the deviations of $\mathrm{RM_i}$ from the model curves originate in the Galactic foreground? For several reasons this possibility seems unlikely:

(a) The background sources 5 C 3.073, 77, 90, and 96, situated outside the main spiral arms, should only be affected by the rotation in the Galactic foreground and an eventual halo of M 31. Their average $\mathrm{RM_{fg}}$ of $-91 \pm 15\,\mathrm{rad\,m^{-2}}$ agrees well with the value of $-88 \pm 2\,\mathrm{rad\,m^{-2}}$ determined by Beck (1982) and used for the model curves in Fig. 7. The RM of the extragalactic radio source closest to M 31, 3 C 13 at $\sim 5°$ distance (Simard-Normandin et al., 1981; Broten et al., 1987), is $-92 \pm 9\,\mathrm{rad\,m^{-2}}$ which also agrees with the value of $\mathrm{RM_{fg}}$ given above suggesting that the rotation in the halo of M 31 plays a minor role.

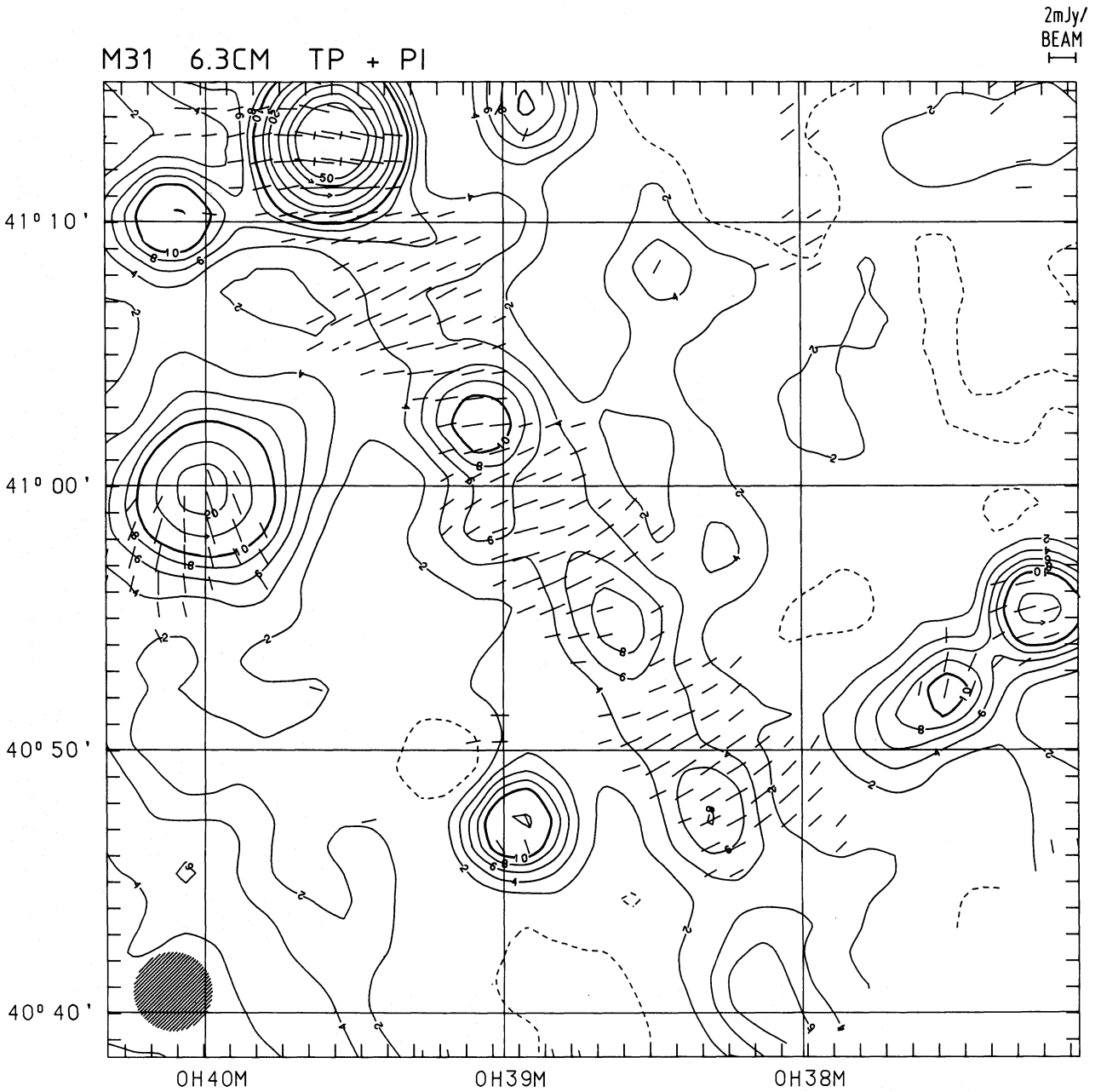

Fig. 3. Total radio continuum emission from the SW spiral arm of M 31 at λ6.3 cm smoothed to a Gaussian half-power beamwidth of 3′ shown in the lower left-hand corner. Contour levels are 0, 1, 2, 3, 4, 6, 8, 10, 15, 20, 30, 40, 50, 100 mJy/beam. The lengths of the *E*-vectors indicate the flux density of the linearly polarized emission

(b) The distribution of Galactic RM indicates that in the direction of M 31 the line of sight makes an angle of $\sim 30°$ to the local field (Broten et al., 1987). Therefore the required $\sim 45\%$ variation of RM_{fg} could only be achieved by a similar variation of the product of the Galactic electron density and the strength of the field component along the line of sight on the scale of our resolution (less than a few parsecs in our Galaxy). However, along the path-length of several kiloparsecs such variations in RM are expected to average out.

(c) The deviations of RM_i from the model curves seem to have similar periods in all four rings (see below). This can hardly be expected from variations originating in the Galactic foreground, and it seems very unlikely that such variations would line up with the spiral arm of M 31.

We conclude from the above that the deviations of RM_i from the model curves in Fig. 7 are indeed originating in M 31. The deviations in the 4 rings are periodic with a "wavelength" in azimuthal angle of 35° to 20° which corresponds to a scale length along the spiral arm of ~ 4.5 kpc at all radii. The effect of a thermal plasma varying in electron density and/or extension along the line of sight, as derived from the thermal radio emission, cannot explain the observations (Fig. 7). The RM_i deviations should then be largest at those positions where $T_{th} \cos(\theta + \phi)$ deviates most strongly from its average value. The data in Fig. 7 do not show such a correlation.

It follows that the periodic deviations of RM_i in Fig. 7 are most probably caused by the field structure within M 31. This result is supported by the variations of the degree of polarization at

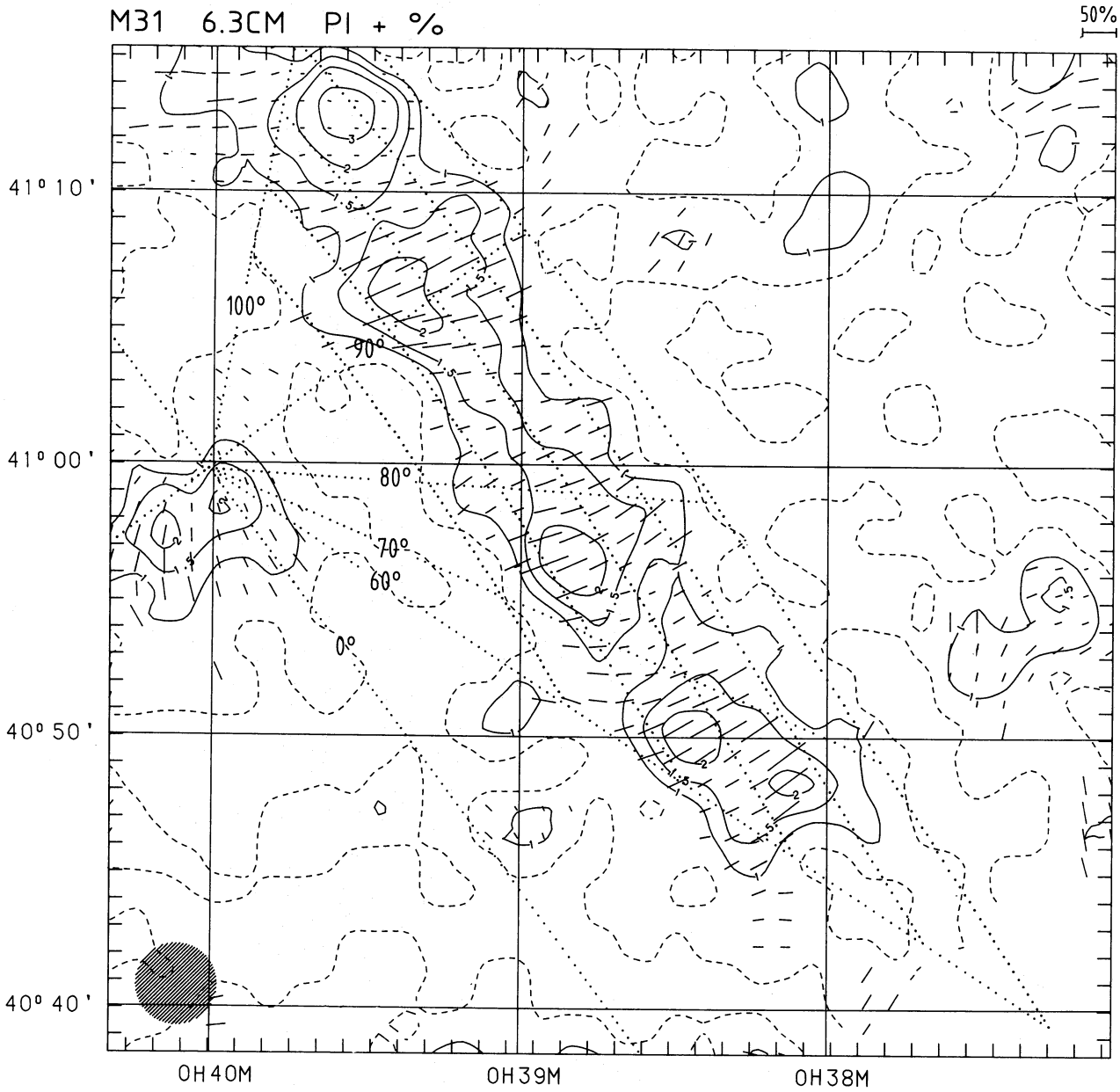

Fig. 4. Linearly polarized emission from the SW spiral arm of M 31 at $\lambda 6.3$ cm smoothed to a half-power beamwidth of 3′. Contour levels are 0, 1, 1.5, 2, 3 mJy/beam. The lengths of the *E*-vectors show the degree of linear polarization. The dotted lines indicate the radii 6, 8, 10, 12, and 14 kpc and the azimuthal angles 0°, ..., 100° in the plane of the galaxy assuming $i = 78°$ and $D = 690$ kpc

$\lambda 6.3$ cm ($p_{6.3}$) in the ring 8–10 kpc where the emission is strongest, and in the ring 10–12 kpc (Fig. 8). The intrinsic degree of polarization is determined by the degree of uniformity of the field component in the plane of the sky ($B_\perp$), but it is reduced by Faraday depolarization if a $B_\parallel$-component exists. In the ring 8–10 kpc (Fig. 8) $p_{6.3}$ varies with a "wavelength" along the spiral arm of $\Delta\theta \simeq 13°$ (2.3 kpc), half the "wavelength" of the RM variation produced by the $B_\parallel$-component. If both effects are due to the same field in M 31 and if the thermal fraction of the total emission is roughly constant as suggested by Beck and Gräve (1982), $p_{6.3}$ should reach a minimum at positions of maximum amplitude of RM_i, regardless of sign, i.e. at $\theta \simeq 60°, 70°, 85°$, and 100°. At the first 3 angles this is indeed observed. The disagreement at $\theta = 100°$ is caused by the polarized source 5 C 3.107, for which RM_i was not corrected.

The observed region is situated near the minor axis where the angle of the axisymmetric field lines with respect to the plane of the sky is small. An additional periodic variation of the field angle in the plane of M 31 in this region of $\leqq 25°$ could explain the RM_i deviations of Fig. 7 (as $RM_{max} \sin 25°/\sin i_0 \simeq 40$ rad m^{-2}, where $RM_{max} = 93$ rad m^{-2} is the maximum intrinsic rotation measure near the major axis (Beck, 1982) and $i_0 = 78°$ the corresponding maximum angle of the axisymmetric field lines with respect to the plane of the sky). The degree of polarization would then be reduced by $\leqq (\cos 25°)^{1-\alpha_n}$ (where α_n is the spectral index of the nonthermal emission). For $\alpha_n \simeq -0.88$ (Beck and Gräve, 1982) p

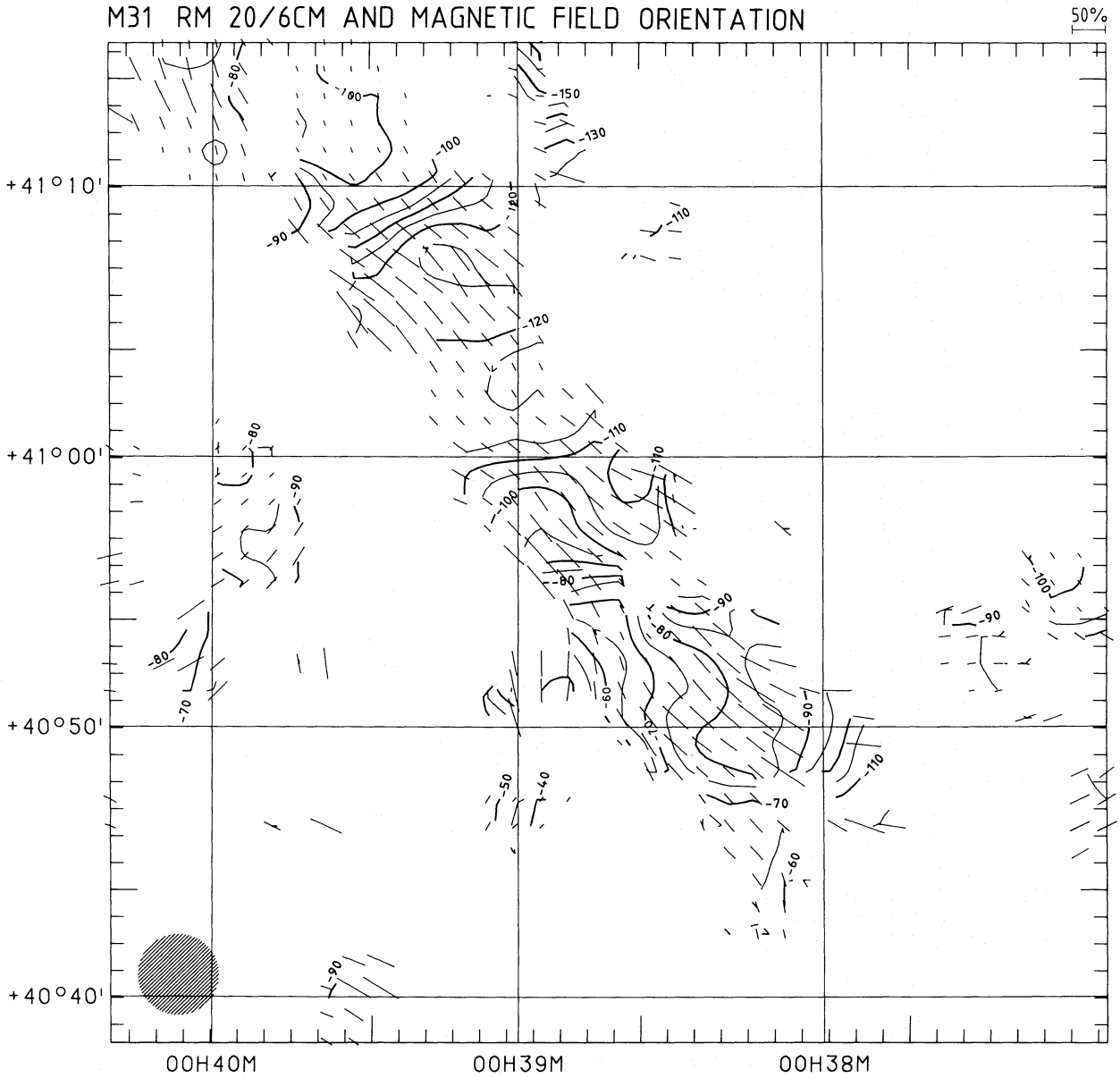

Fig. 5. Distribution of rotation measures RM (in rad m^{-2}) at a resolution of 3′. RM was computed only for points at which the polarized flux densities at λ20.1 and λ6.3 cm are higher than 2 times the rms noise. The vectors indicate the orientations of the magnetic field (χ_B) and have lengths proportional to the degree of linear polarization at λ6.3 cm

is reduced by the inclination effect by a factor 0.83. The observed values of 0.3–0.5 indicate that the contribution of thermal emission to the total emission and the effects of Faraday depolarization or a random component of the magnetic field may be significant; these effects will be discussed in Paper II.

The periodic variations of the field orientation are not restricted to the plane of M 31, but are also visible in the plane of the sky, i.e. nearly perpendicular to the plane of M 31. Figure 9 shows the position angles χ_B of the $B_\perp$ component as a function of azimuthal angle. In a nearly toroidal field χ_B should be $\simeq 37°$ at $\theta = 90°$ and then slowly decrease to $\chi_B = 30°$ at $\theta = 60°$. Instead, we see variations with amplitudes $\sim \pm 30°$ in the ring 6–8 kpc, $\pm 15°$ in the ring 8–10 kpc and $\sim \pm 20°$ in the ring 10–12 kpc. In the ring 6–8 kpc the variation of χ_B is periodic and clearly anticorrelated to that of RM_i (Fig. 7), i.e. the scale length along the arm is again $\sim$4.5 kpc, indicating a *three-dimensional field deviation*. In the ring 8–10 kpc a similar anticorrelation between RM_i and χ_B is visible, except for the region around $\theta = 86°$. In the outer rings no periodicity is seen; here the magnetic field is turning away from the spiral arm at $\theta \lesssim 75°$ (see also Fig. 6), possibly following an interarm segment visible in neutral hydrogen (Brinks and Shane, 1984).

The independent data of RM_i, $p_{6.3}$ and χ_B indicate the existence of a three-dimensional arc-like structure of the magnetic field on a scale of $\sim$4.5 kpc in the plane of M 31, superimposed onto the axisymmetric and possibly a BSS field (Fig. 10). The scale and shape of this structure are reminiscent of the Parker-Jeans instability as discussed by Elmegreen (1982, 1987). In such an instability the magnetic field is tied to the spiral arm at the positions of large cloud complexes and inflated out of the plane in

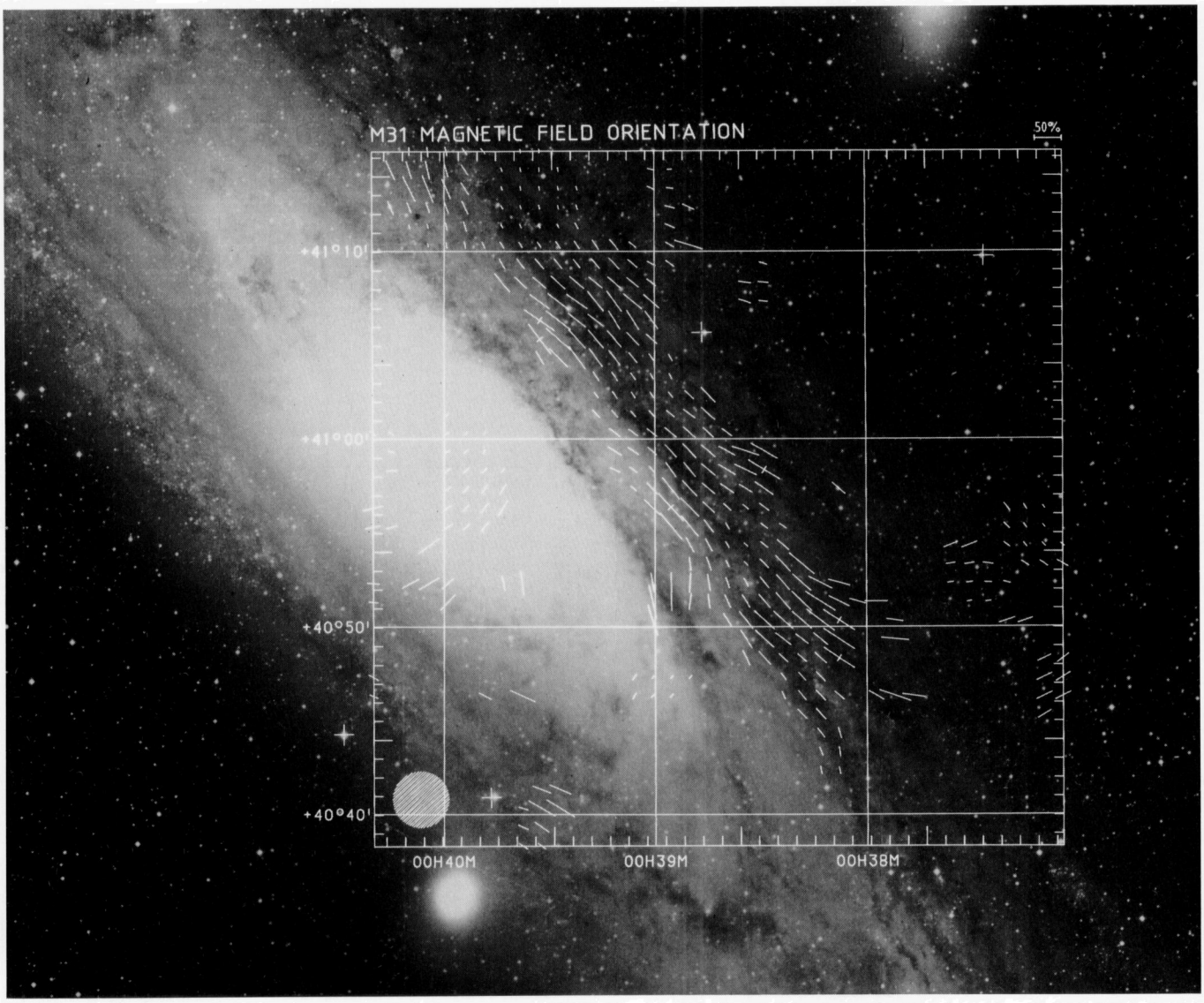

Fig. 6. Orientation of the magnetic field (χ_B) at a resolution of 3′ overlayed onto an optical photograph of the Hale Observatories. The lengths of the vectors indicate the degree of linear polarization at $\lambda 6.3$ cm

between cloud complexes. The arc-like field structure observed between $\theta = 70°$ to $86°$ (compare also Fig. 4) could be anchored in a large H I complex of ~ 2 kpc length visible in the ring 8–10 kpc, between 5′ and 15′ distance from the minor axis, on the map of integrated H I of Brinks and Shane (1984) as presented by Walterbos and Schwering (1987). The central part of this complex is coincident with maxima in polarized intensity and $p_{6.3}$ (Fig. 4) and with values of RM_i agreeing with the model curve (Fig. 7), while at the borders of the H I complex the inflated field lines cause high rotation measures and low values of $p_{6.3}$ (see Fig. 5). Around $\theta = 70°$ a kink in the main H I arm is seen (also visible in the $\lambda 20$ cm total power distribution in Fig. 1) and a weaker H I arm outside the main arm occurs, to which the wavering out of the projected magnetic field lines may be related.

We will search other areas in M 31 for similar signs of interactions between H I complexes and magnetic fields.

5. The central region

Jacoby et al. (1985) showed the existence of spiral arms and filamentary structure in the ionized gas near the centre of M 31. These spiral arms were also detected in the nonthermal radio emission at $\lambda 21$ cm by Walterbos and Gräve (1985). Recently Ciardullo et al. (1988) published a deep Hα+[N II] image of the bulge of M 31. A reproduction of their Fig. 3 b is shown in Fig. 11 with vectors indicating the magnetic field orientation from Fig. 6 superimposed. In the southern part the magnetic field appears to be generally aligned with the spiral arm structure seen in the ionized gas. The same field orientation was obtained by Berkhuijsen et al. (1987) from Effelsberg data at $\lambda 11.1$ cm and $\lambda 6.3$ cm.

Comparison of Fig. 11 with Figs. 2 and 4 shows that both at $\lambda 20.1$ cm and at $\lambda 6.3$ cm maxima of polarized emission coincide with the broad arm seen nearly face-on at 2′ south and east of the

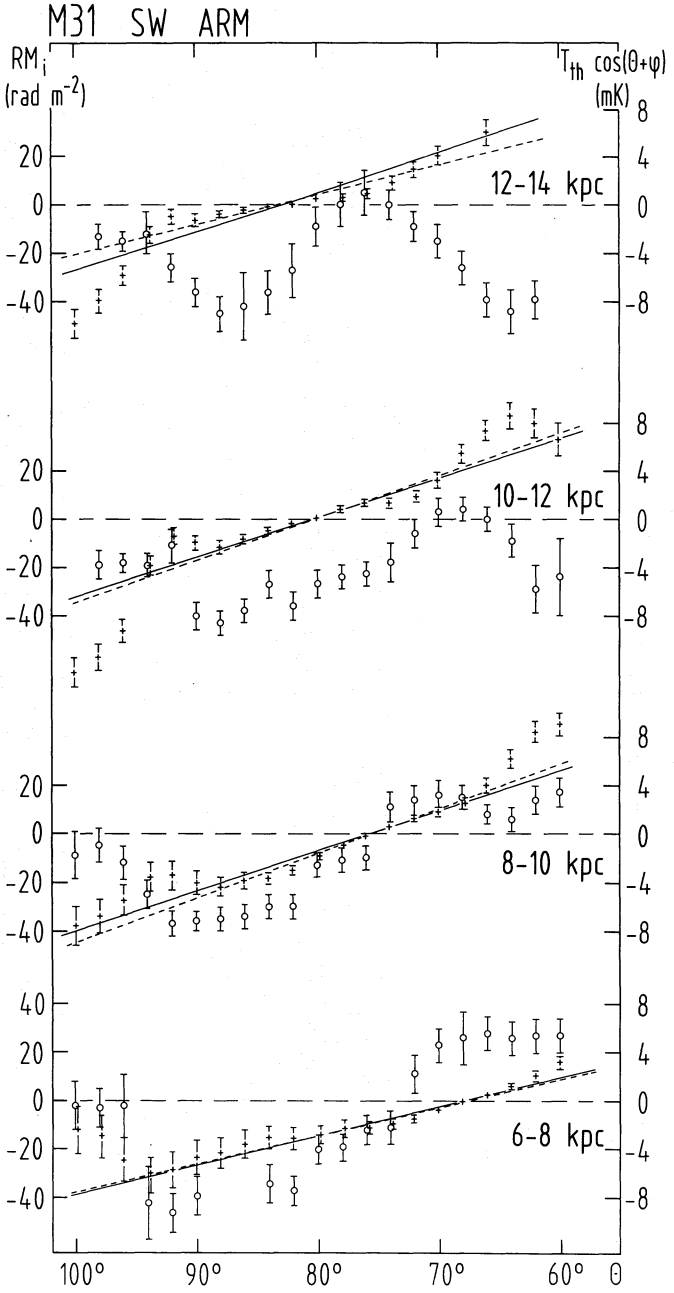

Fig. 7. Average rotation measures intrinsic to M 31 (open circles) in 4 different radius intervals in sectors of 2° width in azimuthal angle in the plane of the galaxy. A foreground rotation measure $RM_{fg} = -88\,rad\,m^{-2}$ was subtracted (Beck, 1982). The full lines indicate the variation of RM_i predicted by the axisymmetric field model of Beck (1982). The following interpolated values of RM_{max} and ϕ [Eq. (1)] were used: $RM_{max} = 66, 97, 106, 92\,rad\,m^{-2}$ and $\phi = 22°0$, 14°5, 9°5, 7°2 for the rings 6–8, 8–10, 10–12, 12–14 kpc, respectively. The crosses give the thermal emission obtained by Beck and Gräve (1982) averaged in sectors and scaled by $\cos(\theta + \phi)$ to include the geometric variation of the model component $B_{\parallel}$. The dashed line shows the geometric variation for constant thermal emission equal to the mean emission of all sectors

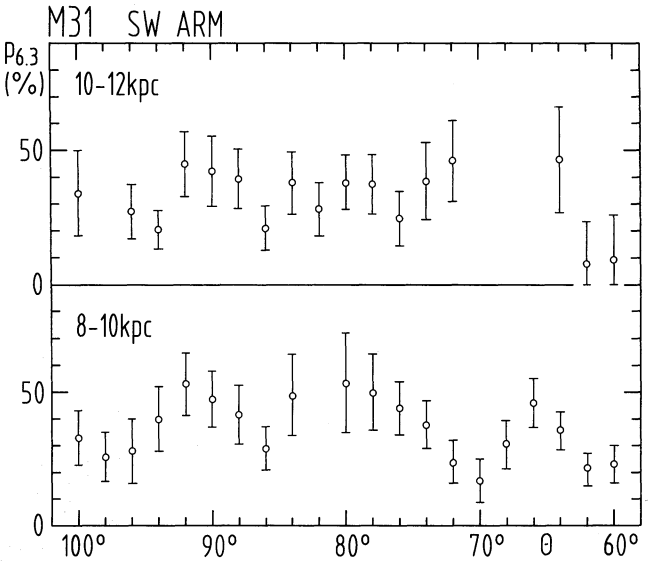

Fig. 8. Degree of polarization at $\lambda 6.3$ cm in two radius intervals averaged in sectors in the plane of the galaxy of 2° width in azimuthal angle. Eight total power sources (5C 3.73, 88, 90, 94, 97, 98, 99, and 107) and one polarized source (5C 3.107) were subtracted

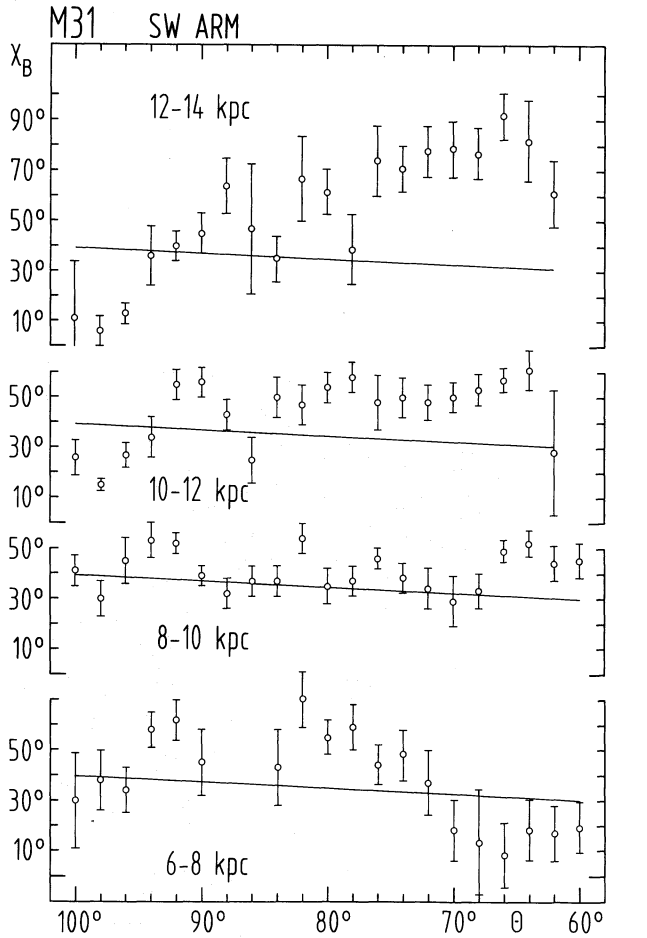

Fig. 9. Position angles χ_B of the magnetic field averaged in the same sectors as in Fig. 7. The line shows the variation expected for the axisymmetric field component

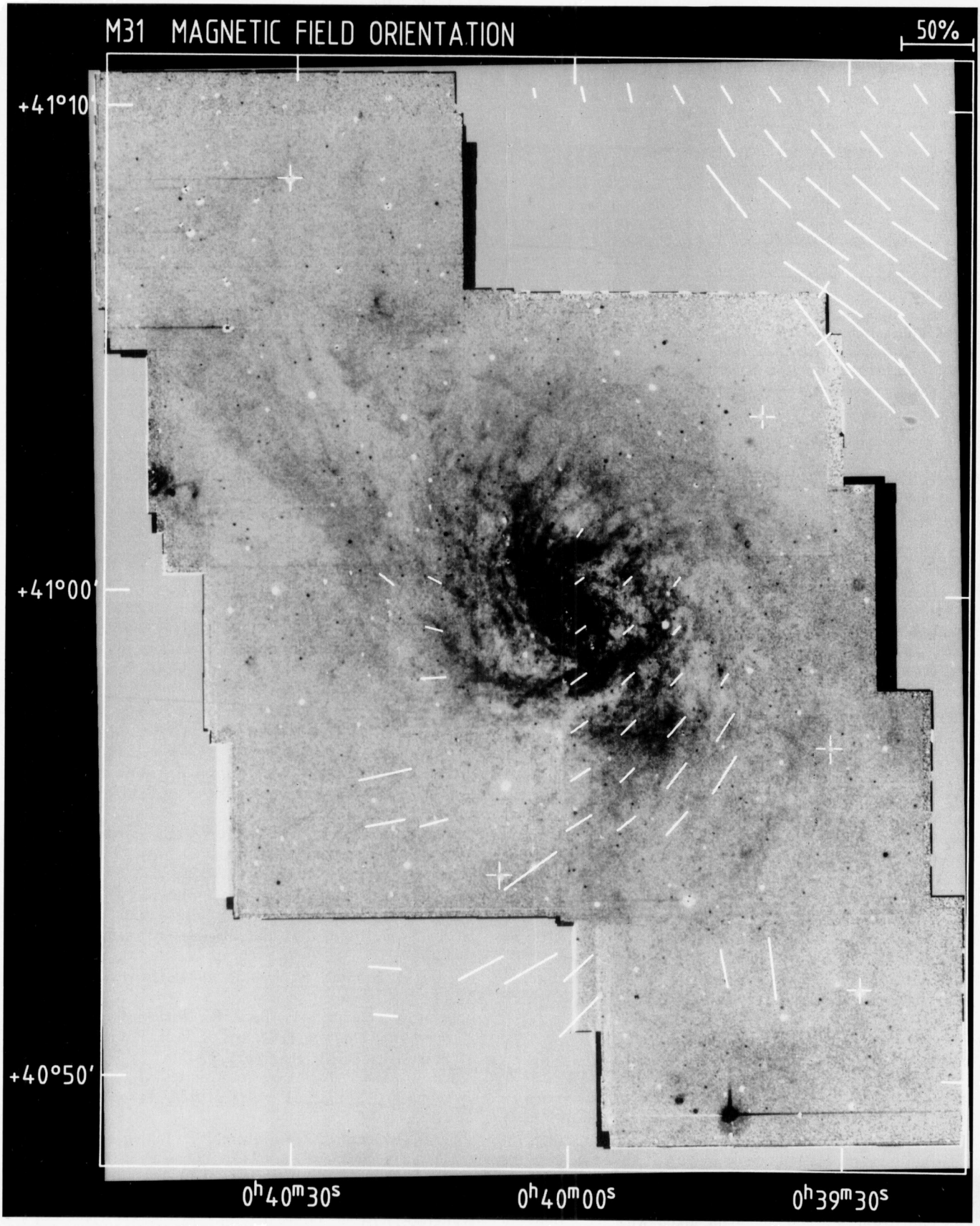

Fig. 11. Orientation of the magnetic field (χ_B) in the central region of M31 overlayed onto the Hα photograph of Ciardullo et al. (1988). The lengths of the vectors indicate the degree of linear polarization at λ6.3 cm

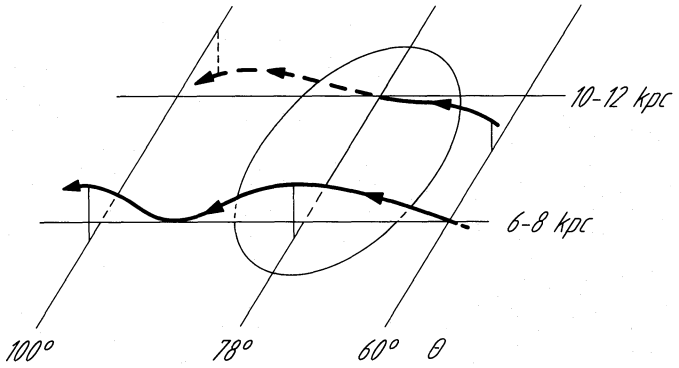

Fig. 10. Sketch of the three-dimensional field structure along the spiral arm as implied by the data in Fig. 7 and 9. The straight lines, indicating the azimuth θ and the position of two rings, are in the plane of M 31. In the ring 6–8 kpc the field runs upwards and towards us between $\theta = 60°$ and $\theta \simeq 78°$ ($RM_i > 0$), from where it bends over to run downwards and away from us up to $\theta \simeq 95°$ ($RM_i < 0$), from where it again comes upwards and towards us. In the ring 10–12 kpc the field runs downwards and away from us between $\theta = 60°$ and $\theta \simeq 95°$ ($RM_i < 0$) from where it comes upwards and towards us ($RM_i > 0$). The ellipse indicates the approximate position of the H I complex. The field is thought to be anchored in the H I cloud around $\theta \simeq 78°$ and is inflated on either side. The field line drawn in the 6–8 kpc ring should also run in the plane of M 31 at $\theta = 78°$, but was sketched above this plane for clarity. Of course, in reality the H I cloud, the spiral arm and the magnetic field structure have considerable thickness perpendicular to the plane of M 31

nucleus. At λ 20.1 cm the polarized emission is confined to the bright ionized features, but at λ 6.3 cm polarized emission comes also from positions in between the arms indicating that diffusion of relativistic electrons into interarm regions takes place.

North of $\delta = +41°$ no polarized emission at λ 20.1 cm is found and only very weak emission at λ 6.3 cm. In this area the ionized gas layer has an inclination of $\simeq 45°$, and a very filamentary and complex structure suggesting that variations in rotation measure across the beam may cause the depolarization. Ciardullo et al. (1988) estimate a width of the filaments of $\lesssim 20$ pc. Assuming that half of the area of the 3′ beam is filled with filaments, the number of filaments per beam area at a distance of 690 kpc is $\gtrsim 15$. With a dispersion in RM of 140 rad^2 m^{-4} the degree of polarization at λ 6.3 cm would drop to $\lesssim 20\%$, while that at λ 20.1 cm would be wiped out completely. On the other hand, a possible warp in the filamentary structure noted by Ciardullo et al. (1988) could also have a depolarizing effect because of a tangled structure of the magnetic field in the line of sight.

Observations at $\lambda \lesssim 6$ cm with higher resolution are required to reveal the field structure in the central area of M 31.

6. Conclusions

Observations at λ 20.1 cm with the VLA centred on an area of high polarized emission near the minor axis in the SW arm of M 31 revealed variations in polarization angle and percentage of polarization on the scale of the beamwidth of 250 × 1250 pc in the plane of M 31 (Fig. 2). The polarized emission is concentrated on a dust lane running just outside the optically brightest spiral arm.

Comparison with λ 6.3 cm data taken with the Effelsberg telescope (Berkhuijsen et al., 1987) permitted the following conclusions:

1. Both the rotation measures (RM) and the intrinsic magnetic field orientations (χ_B) confirm the model of a basic axisymmetric, nearly toroidal field in M 31.

2. Periodic deviations from the basic mode along the "ring" of emission (i.e. in azimuthal angle) are present in both the intrinsic rotation measure (RM_i) and χ_B which also affect the degree of polarization ($p_{6.3}$). Their typical scale length along the arm is ~4.5 kpc.

3. The deviations in RM_i and the variations in $p_{6.3}$ cannot be explained by the distribution of thermal electrons along the arm. As it is also unlikely that the deviations in RM_i and χ_B originate in the Galactic foreground, we conclude that they are caused by a three-dimensional, arc-like structure of the magnetic field in M 31, possibly a Parker-Jeans instability anchored in a large H I complex (see Fig. 10). It is the first time that such an instability is directly observed.

4. In the central area of M 31 the magnetic field is oriented along the spiral arms seen in the ionized gas to the south of the nucleus (Fig. 11). On the northern side the polarized emission at λ 20.1 cm is completely wiped out, possibly because of a filamentary or warped structure of the magnetic field.

Acknowledgements. We thank Dr. R. Ciardullo for a photograph of the central area of M 31 and a list of star positions, which enabled us to make the overlay shown in Fig. 11. We are grateful to Dr. M. Krause for valuable comments on the manuscript.

References

Beck, R.: 1982, *Astron. Astrophys.* **106**, 121
Beck, R., Gräve, R.: 1982, *Astron. Astrophys.* **105**, 192
Beck, R., Berkhuijsen, E.M., Wielebinski, R.: 1980, *Nature* **283**, 272
Berkhuijsen, E.M., Beck, R., Gräve, R.: 1987, in *Interstellar Magnetic Fields*, eds. R. Beck, R. Gräve, Springer, Berlin, Heidelberg, New York, p. 38
Brinks, E., Shane, W.W.: 1984, *Astron. Astrophys. Suppl.* **55**, 179
Broten, N.W., MacLeod, J.M., Vallée, J.P.: 1987, *Astrophys. Space Sci.* **141**, 303
Ciardullo, R., Rubin, V.C., Jacoby, G.H., Ford, H.C., Ford, W.K.: 1988, *Astron. J.* **95**, 438
Elmegreen, B.G.: 1982, *Astrophys. J.* **253**, 655
Elmegreen, B.G.: 1987, *Astrophys. J.* **312**, 626
Georgiev, T.B.: 1988, *Sov. Astron. Lett.* **14**, 53
Jacoby, G.H., Ford, H., Ciardullo, R.: 1985, *Astrophys. J.* **290**, 136
Krause, M., Hummel, E., Beck, R.: 1989, *Astron. Astrophys.* **217**, 4
Loiseau, N., Hummel, E., Beck, R., Wielebinski, R.: 1987, in *Interstellar Magnetic Fields*, eds. R. Beck, R. Gräve, Springer, Berlin, Heidelberg, New York, p. 42
Pellet, A., Astier, N., Viale, A., Courtès, G., Maucherat, A., Monnet, G., Simien, F.: 1978, *Astron. Astrophys. Suppl.* **31**, 439
Simard-Normandin, M., Kronberg, P.P., Butten, S.: 1981, *Astrophys. J. Suppl.* **45**, 97
Sofue, Y., Takano, T.: 1981, *Publ. Astron. Soc. Japan* **33**, 47
Sofue, Y., Beck, R.: 1987, *Publ. Astron. Soc. Japan* **39**, 541
Walterbos, R.A.M., Gräve, R.: 1985, *Astron. Astrophys.* **150**, L 1
Walterbos, R.A.M., Schwering, P.B.W.: 1987, *Astron. Astrophys.* **180**, 27